NANO LETTERS
Letter
pubs.acs.org/NanoLett

Nanoscale Plasmonic Memristor with Optical Readout Functionality

Alexandros Emboras, Ilya Goykhman, Boris Desiatov, Noa Mazurski, Liron Stern, Joseph Shappir, and Uriel Levy*

Department of Applied Physics, The Benin School of Engineering and Computer Science, The Center for Nanoscience and Nanotechnology, The Hebrew University of Jerusalem, Israel, 91904

ABSTRACT: We experimentally demonstrate for the first time a nanoscale resistive random access memory (RRAM) electronic device integrated with a plasmonic waveguide providing the functionality of optical readout. The device fabrication is based on silicon on insulator CMOS compatible approach of local oxidation of silicon, which enables the realization of RRAM and low optical loss channel photonic waveguide at the same fabrication step. This plasmonic device operates at telecom wavelength of 1.55 μm and can be used to optically read the logic state of a memory by measuring two distinct levels of optical transmission. The experimental characterization of the device shows optical bistable behavior between these levels of transmission in addition to well-defined hysteresis. We attribute the changes in the optical transmission to the creation of a nanoscale absorbing and scattering metallic filament in the amorphous silicon layer, where the plasmonic mode resides.

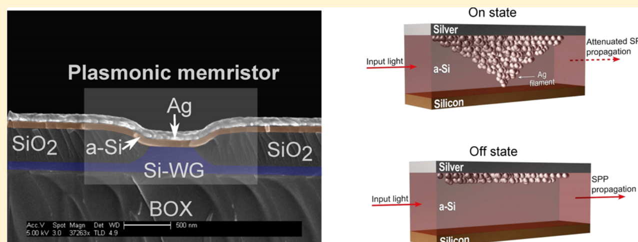

KEYWORDS: *Local oxidation, resistive memories, memristor, silicon-photonics, surface-plasmons*

Resistive random access memory (RRAM) technology is considered as a promising candidate for next-generation nonvolatile memories.[1] This new class of devices consists of a simple metal−insulator−metal (MIM) layer structure, and the principle of operation is based on the switching of the electrical resistance between two levels, a low-resistance state and a high-resistance state. Among numerous demonstrations in the literature,[2−5] much attention has been focused on conductive bridge (CB) cells[6] due to their outstanding performance (i.e., low switching electrical power, endurance, retention, high speed, and high scalability) and easy CMOS integration (simple materials and structure). In this CB-RRAM technology, the resistance switching can be achieved through the formation/annihilation of the nanoscale metal filament under the appropriate electrical conditions.

The introduction of photons inside the RRAM memristive devices and the subsequent electro-optical interaction could be very beneficial in the context of memory performances. For example, Ungureanu et al.[7] demonstrated a RRAM device consisting of a four-layer Pd−Al_2O_3−SiO_2−Si memory cell, where its resistance state was controlled through the light-induced photogenerated current on Si/SiO_2 interface, providing multibit operation. In a very recent publication, Park et al.[8] present a CB-RRAM device based on ZnO nanorods system where the filament annihilation and generation was strongly correlated with the optical excitation conditions. Although their findings open a new paradigm for application of RRAM in photonic devices, to the best of our knowledge, the integration of RRAM devices within a photonic or a plasmonic circuitry has not yet been experimentally demonstrated.

We experimentally demonstrate a nanoscale CB-RRAM memristive device integrated with an silicon on insulator (SOI) waveguide for the purpose of optical readout at telecommunication wavelengths. The device is fabricated using the CMOS compatible approach of local-oxidation of silicon (LOCOS), which limits the lateral misalignment between the SOI waveguide and the active device.[9] This CB-RRAM cell is written and erased electrically and read optically by measuring two different level of transmission. The electro-optical measurements show an optical hysteresis with an off/on optical transmission ratio of few percent. This optical method to read RRAM devices has the potential of becoming an important building block in future optoelectronic system, as it may reduce the numbers of optical to electrical conversions.[10]

The optically readable CB-RRAM memristive device investigated in this paper is schematically depicted in Figure 1. It consists of a vertical Ag/a-Si/p-Si structure butt-coupled to a single-mode SOI waveguide with a 280 nm × 350 nm cross section (Figure 1a). The silicon channel waveguide serves as the medium of propagating light. As the light propagates through the CB-RRAM devices, it couples mainly to the fundamental plasmonic mode, which is highly confined at the Ag/a-Si interface.[11] The optical transmission via the CB-RRAM memristive device can be varied by switching the electrical resistance of a-Si, where the switching mechanism originates by the formation/annihilation of nanoscale silver filaments.[12−14] Shortly, under the application of positive voltage at the silver electrode, silver ions are diffused inside the a-Si and trapped in defect sites. The recombination of silver ions with electrons coming from the substrate leads to the construction of

Received: September 18, 2013
Revised: November 16, 2013
Published: November 20, 2013

Downloaded via HEBREW UNIV OF JERUSALEM on July 31, 2020 at 18:13:15 (UTC).
See https://pubs.acs.org/sharingguidelines for options on how to legitimately share published articles.

© 2013 American Chemical Society

dx.doi.org/10.1021/nl403486x | *Nano Lett.* 2013, 13, 6151−6155

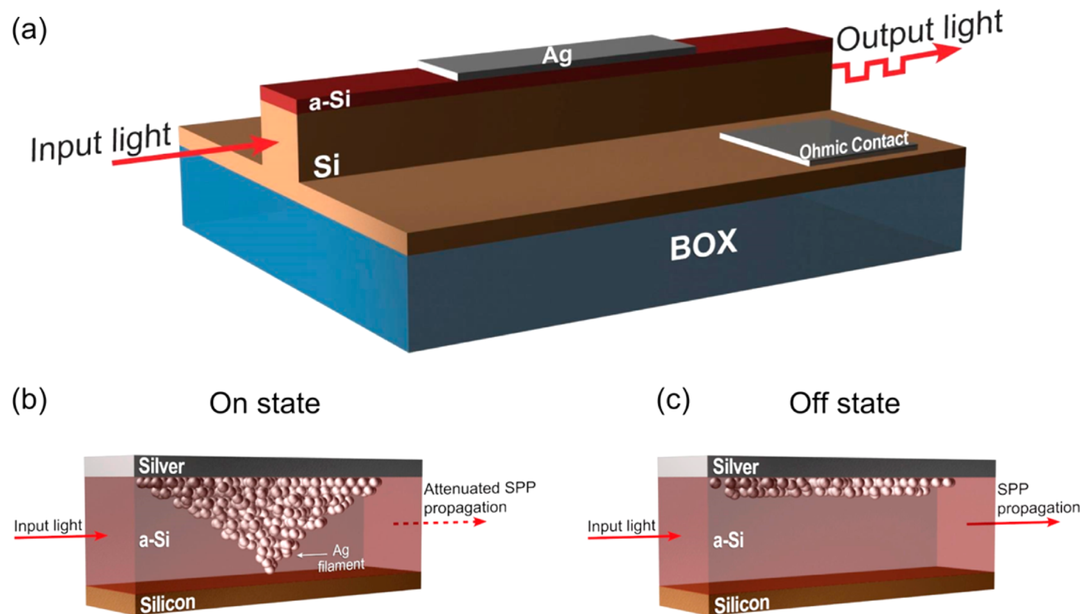

Figure 1. (a) Three-dimensional schematic of the investigated optically readable plasmonic RRAM. (b) Formation of the nanoscale filament in the on state. (c) Annihilation of the nanoscale filament in the off state.

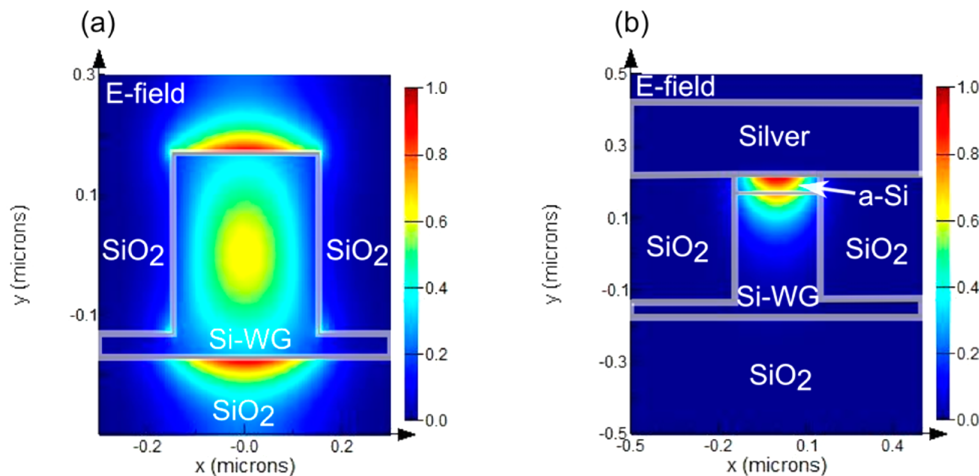

Figure 2. (a) Calculated E field intensity of the fundamental TM-like mode supported by the SOI-WG. (b) Calculated E field intensity of the fundamental mode supported by the RRAM-memristive device. The E field intensity is defined as the sum of the amplitude squares of all electric-field components, that is, $|E|^2 = |Ex|^2 + |Ey|^2 + |Ez|^2$.

nanoscale chain of silver nanoparticles (Figure 1b), and the conduction mechanism is dominated by an enhanced electron tunneling through this metal filament (low resistance state); that is, the device is turned on and the measured optical transmission is low. When a negative voltage is applied, the metal filament is dissociated (Figure 1c) and the tunneling rate of electrons is greatly reduced (high resistance state); that is, the device is turn off and the measured optical transmission is high. By taking advantage of the voltage-induced changes in the nanoscale metal filament, we are able to optically read the electrical state of the device as a result of the variation of the absorption and scattering loss of the fundamental plasmonic mode.

Next, we perform 3-D electromagnetic full wave simulations to find the modes that are supported by our structure. We use the following values of refractive index: 1.44 (SiO_2), 3.48 (Si), 0.14 + 11.4i (Ag, as given by Johnson and Christy[15]), and an a-Si refractive index of 3.3 at 1550 nm based on our ellipsometry measurements. By using a modal analysis (Lumerical FDTD), we found that the RRAM memristor supports the fundamental plasmonic mode having most of its energy resides in the a-Si layer (Figure 2b), with an effective index of $n_{RRAM} = 3.32$ and propagation losses of 0.24 dB/μm. Then, we investigate the coupling efficiency between the silicon waveguide and the RRAM memristor. On the basis of the direct coupling theory,[16] the expected power transmission between the fundamental TM-like SOI-WG mode (Figure 2a) with an effective index of $n_{SiWG} = 1.9$ and the fundamental plasmonic mode of the RRAM memristor is the product of the Fresnel transmission coefficient multiplied by the overlap integral of the corresponding modes field, which is estimated to be 64%. On the basis of these values, the insertion loss of the RRAM memristor, which is given as the sum of the coupling loss (two interfaces) and the propagation loss, is estimated to be 4.2 dB. One should note that this insertion loss can be further improved by reducing the coupling

dx.doi.org/10.1021/nl403486x | *Nano Lett.* 2013, 13, 6151−6155

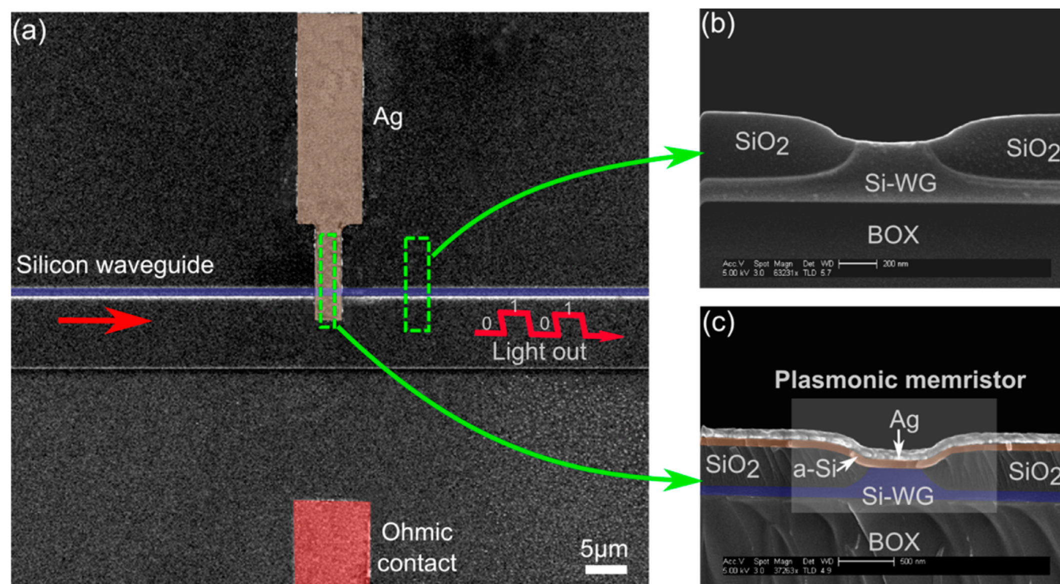

Figure 3. (a) Scanning electron microscope (SEM) micrograph showing the top view of the fabricated plasmonic RRAM structure integrated with the SOI waveguides. (b) SEM image of the cross section of the LOCOS waveguide. (c) SEM image of the cross section of the optically readable memristive RRAM.

loss between the photonic mode and the plasmonic mode using adiabatic or non adiabatic approaches; see, for example, ref 17.

The optically readable plasmonic RRAM device and its integrated photonic waveguides were fabricated on a 340 nm thick p-type silicon device layer (ρ = 0.024 Ω.cm) on top of a 2 μm thick buried oxide. The SOI waveguides were fabricated using the CMOS-compatible approach of LOCOS.[18] First, a 100 nm thick silicon nitride (SiN) was deposited on the silicon by plasma-enhanced chemical vapor deposition (PECVD) at 300 °C to realize a protective layer for the LOCOS process. Next, the mask defining the optical and electrical structures including the photonic bus waveguide, the RRAM region, and the contacts area was patterned using standard electron-beam lithography (EBL). The pattern was transferred to the protective SiN layer by reactive ion etching (RIE) with a CHF_3/O_2 gas mixture. The defined pattern was next transferred to the silicon layer by wet oxidation process at 1000 °C with the nitride layer serving as a mask preventing the oxygen diffusion. To be able to form the RRAM region, we removed the nitride mask by wet etching in hot phosphoric acid. To integrate the RRAM device, we first contacted the Si rib waveguide by aluminum pad and alloyed the structure by heating to 420 °C under H_2/N_2 ambient condition to ensure ohmic behavior. Next, the active layer was formed by depositing 50 nm of a-Si using PECVD (SiH_4:Ar = 50 sccm:500 sccm at 200 °C, 10 mTorr). A 2 μm wide silver strip (100 nm thick) intersecting the SOI waveguide was formed by metal evaporation and lift-off. An optical microscope image showing the top view of the final device is shown in Figure 3a. Cross sections of the fabricated LOCOS waveguide and the memristor region captured by scanning electron microscope are shown in Figure 3b,c, respectively.

To investigate the electrical resistance switching behavior of the fabricated memristor device, we measured the DC leakage current at different voltages. $I-V$ measurements were performed using a Keithley 4200 semiconductor characterization system. The bias voltage was applied to the top metal (Ag), while the back contact (p-Si) was grounded. Figure 4 shows four consecutive $I-V$ switching characteristics of the investigated optical CB-RRAM memristive device. A high degree of repeatability and a well-defined hysteresis are demonstrated by the multiple switching $I-V$ curves. Because the voltage is increased above a threshold voltage, the device is turned on and the conductance is increased very rapidly. This region of the curve defines the "threshold switching phenomena" and is attributed to the formation of silver filament,[19−21] while the region before the threshold voltage defines the "subthreshold switching phenomena". The device is turned off and the conductance reduced abruptly for small negative voltage. The switching threshold voltage and current observed in this study was 4.5 V and 35 nA, respectively, which are in fair agreement with the values published elsewhere.[22] The small difference can be attributed to different fabrication conditions of the deposited a-Si. On the basis of these numbers, the switching power is on the order of 0.15 μW. Considering the potential of operation rates approaching the gigahertz, these power levels indicate the possibility of achieving switching energies in the femtojoule per bit regime. Next, we investigated the conduction mechanism through the a-Si layer by measuring the DC leakage current at different temperatures. The investigation was performed at the regime of the "subthreshold

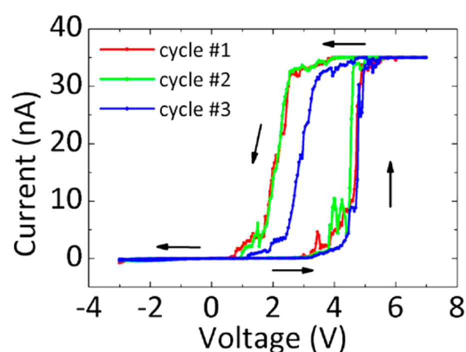

Figure 4. $I-V$ switching characteristics of the nanoscale optical RRAM device consist of Ag/a-Si/pSi layer fabricated on SOI wafer.

dx.doi.org/10.1021/nl403486x | Nano Lett. 2013, 13, 6151−6155

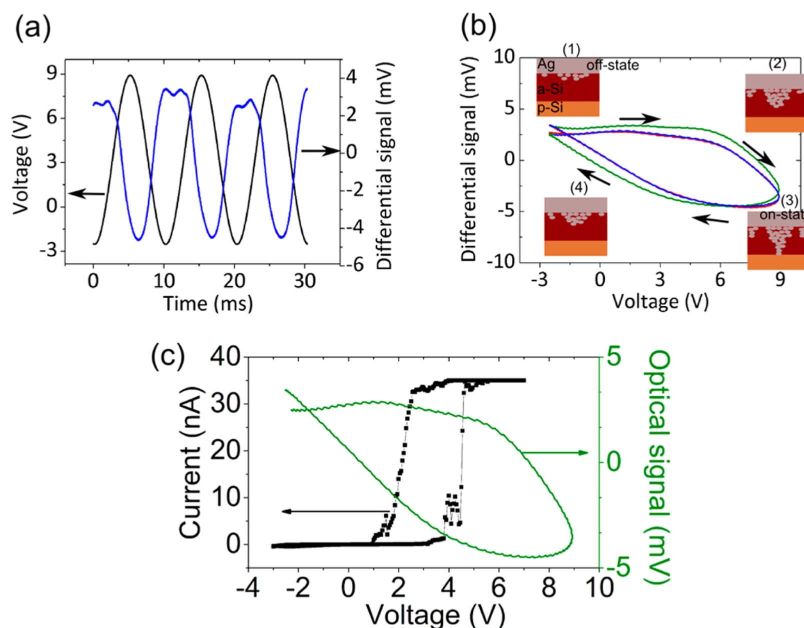

Figure 5. (a) Applied voltage (black) and the resulting differential signal (blue) as a function of time. The differential signal represents the optical modulation values measured by the photodetector, after eliminating the background level via the use of AC coupling mode. (b) Differential signal as a function of the voltage demonstrating the optical switching characteristics of the optical RRAM. (c) Leakage current and optical signal as a function of the voltage, plotted in the same graph.

switching phenomena" to avoid undesired semipermanent changes of its phase state, which may occur during the "threshold switching phenomena". We observed two different conduction mechanisms, which are field-dependent: an ohmic-like conduction for low fields[23] and an enhanced conduction starting at ~1.5 V. The latter is well-fitted to Poole−Frenkel (PF) emission for nonisolated trap[24] with extracted activation energy of 0.7 eV.[25]

The previously mentioned electrical characterization indicates that the Ag/a-Si/pSi CB-RRAM cell is indeed a reliable electrical switching resistance device, as expected. The significant difference between our device and the conventional electrical RRAM[22] is that our device uses the p-Si layer not only as an electrode but also as a medium that supports the propagation of plasmonic and photonic signals. This novel approach allows the investigation and demonstration of new functionalities such as optical readout of the memory logic state. To demonstrate the capability of optical readout, we characterized the behavior of the optical CB-RRAM by measuring the optical transmission at different electrical bias conditions. A diode laser source at 1500 nm wavelength coupled to a polarization maintaining single mode fiber was used to excite the TM-like fundamental mode inside the SOI waveguide. A similar fiber was placed at the output facet, and the transmission through the device was measured using an InGaAs photodetector. A function generator is used to apply an electrical signal to the device. In the specific measurements reported here, a DC-biased (bias of 3 V) sine wave with a frequency of 100 Hz and amplitude of 6 V was applied to the device. As shown in the next section, such variation of the voltages was sufficient for achieving electrical write/erase of the device. The output optical modulated signal was detected by a photodetector that was connected to a digital oscilloscope (DSO-X 2001A). The observed modulation depth of the optical signal was on the order of 1%. Therefore, an AC coupling mode was used to improve the signal-to-noise ratio. It is worth noting that the value of the modulation depth it is expected to be improved in the case that we consider a plasmonic or optical cavity due to the significant field and absorption enhancements within the aSi, where the silver nanofilaments resides.

Figure 5a shows the measured time-dependent differential signal, which correspond to the optical signal measured by the photodetector, as a function of the applied voltages for few consecutive voltage sweeps. By applying a write voltage of 9 V, the device is switched on and the differential signal is reduced. After the application of an erase voltage of −3 V, the signal increases to its initial value. By monitoring the high or low differential signal, we can identify the logic state of the device and therefore optically read the CB-RRAM. It is worth noting that while the write/erase operation speed of our device was estimated to be a few kilohertz, the operation speed can be enhanced significantly by reducing the resistance and the capacitance of the device. Indeed, the effect can be used for much faster operation speeds in the nanoseconds regime, as shown by ref 26.

To further investigate the electro-optical bistable functionality of our plasmonic memristor device, we recorded the optical differential signal while the voltage sweeps from −3 to 9 V (Figure 5b). A clear and distinct hysteresis is observed. To the best of our knowledge, it is the first time that such hysteresis is demonstrated in CB-RRAM memristive devices. The initial state of the device was set to "off" by applying an erase pulse of −3 V. As the voltage increases, the differential signal is slightly reduced up to the threshold voltage of ~5 V, followed by a more abrupt change (reduction of the differential signal) at higher voltages. By reducing the applied voltage from its maximal value of 9 V, the measured optical signal is gradually increased until the voltage reaches the level of the off state (at V = −3 V), yet during the procedure of voltage reduction, the measured differential signal is lower compared with that measured during the voltage increase step. Therefore, a clear

hysteresis is formed and the transmission of light is smaller. Thus a memory device with electrical write and optical read characteristics is formed. In contrast with previously demonstrated electric write optical read devices[27] where the change in optical transmission was stimulated by the elasto-optic effect, here we use the concept of plasmonic guiding, offering the potential of miniaturization and dense integration. We also note that similarly to the results in Figure 4 where the electrical switching resistance experienced abrupt changes at the threshold voltage, the optical transmission intensity also shows an abrupt reduction at similar values of voltage. Additionally, the differential signal in the "subthreshold switching region" is changing with a more gradual slope compared with the "threshold switching region" in consistency with the observed variations of the electrical resistance during the electrical switching operation (Figure 4).

In conclusion, we have demonstrated an efficient approach to read the logic state of a nanoscale CB-RRAM memristive device optically by monitoring the states of low and high optical transmission. The CB-RRAM was successfully integrated with an SOI waveguide using the LOCOS technique, which is fully compatible with the CMOS technology. The device shows optical bistable behavior with an off/on ratio of few percent, which is attributed to the variation of the absorption and scattering loss of the fundamental plasmonic mode supported by CB-RRAM structure as a result of the filament formation. Switching between off and on states is achieved by voltage-induced annihilation/formation of the nanoscale metal filament inside a thin layer of a-Si, where the plasmonic mode resides. The off/on ratio can be further enhanced by implementing structures such as cavities, which can increase the interaction of light with the lossy metal filament. Finally, while the current work is based on the formation of Ag nanofilaments, other metals such as copper, nickel, aluminum, and chromium can be considered as well.[5] Incorporating such metals into our device may be preferable from the fabrication point of view, paving the way for a CMOS-compatible process, which is essential for future integration of such devices with other electronic and optoelectronic functionalities.

■ AUTHOR INFORMATION

Corresponding Author

*E-mail: ulevy@mail.huji.ac.il.

Notes

The authors declare no competing financial interest.

■ ACKNOWLEDGMENTS

We acknowledge the technical support of Maurice Saidian and Doron Greental. The devices were fabricated at the Center for Nanoscience and Nanotechnology, The Hebrew University of Jerusalem. I.G. and B.D. acknowledge the support of the Eshkol fellowship. The work was partially supported by the US-Israel binational science foundation (BSF).

■ REFERENCES

(1) Lai, S. *IEDM Tech.* **2008**, 1−6.

(2) Perniola, L.; Sousa, V.; Fantini, A.; Arbaoui, E.; Bastard, A.; Armand, M.; Fargeix, A.; Jahan, C.; Nodin, J-F; Persico, A.; Blachier, D.; Toffoli, A.; Loubriat, S.; Gourvest, E.; Beneventi, G. B.; Feldis, H.; Maitrejean, S.; Lhostis, S.; Roule, A.; Cueto, O.; Reimbold, G.; Poupinet, L.; Billon, T.; De Salvo, B.; Bensahel, D.; Mazoyer, P.; Annunziata, R.; Zuliani, P.; Boulanger, F. *IEEE Electron Device Lett.* **2010**, *31*, 488−490.

(3) Yang, J. J.; Pickett, M. D.; Li, X.; Ohlberg, D. A. A.; Stewart, D. R.; Williams, R. S. *Nat. Nanotechnol.* **2008**, *3*, 429−433.

(4) Jung, K.; Seo, H.; Kim, Y.; Im, H.; Hong, J.; Park, J.-W.; Lee, J.-K. *Appl. Phys. Lett.* **2007**, *90*, 052104.

(5) Waser, R.; Dittmann, R.; Staikov, G.; Szot, K. *Adv. Mater.* **2009**, *21*, 2632−2663.

(6) Kund, M.; Beitel, G.; Pinnow, C.-U.; Rohr, T.; Schumann, J.; Symanczyk, R.; Ufert, K.-D.; Muller, G. *IEDM Tech. Dig.* **2005**, 754.

(7) Ungureanu, M.; Zazpe, R.; Golmar, F.; Stoliar, P.; Llopis, R.; Casanova, F.; Hueso, L. E. *Adv. Mater.* **2012**, *24*, 2496−2500.

(8) Park, J.; Lee, S.; Yong, K. *Nanotechnology* **2012**, *23*, 385707.

(9) Goykhman, I.; Desiatov, B.; Khurgin, J.; Shappir, J.; Levy, U. *Nano Lett.* **2011**, *11*, 2219−2224.

(10) Barrios, C.; Lipson, M. *J. Lightwave Technol.* **2006**, *24*, 2898−2905.

(11) Dionne, J. A.; Sweatlock, L. A.; Atwater, H. A.; Polman, A. *Phys. Rev. B* **2005**, *72*, 075405.

(12) Owen, A. E.; Hu, J.; Hajto, J.; Snell, A. *Proc. - Int. Conf. Solid-State Integr. Circuit Technol.* **1998**, 830−833.

(13) Avila, A.; Asomoza, R. *Solid-State Electron.* **2000**, *44*, 17−27.

(14) Yang, Y. C.; Gao, P.; Gaba, S.; Chang, T.; Pan, X.; Lu, W. *Nat. Commun.* **2012**, *3*, 732.

(15) Johnson, P. B.; Christy, R. W. *Phys. Rev. B* **1972**, *6*, 4370.

(16) Snyder, A.; Love, J. *Optical Waveguide Theory*; Science paperbacks *190*; Chapman and Hall: New York, 1983.

(17) Ginzburg, P.; Arbel, D.; Orenstein, M. *Opt. Lett.* **2006**, *31*, 3288−3290.

(18) Desiatov, B.; Goykhman, I.; Levy, U. *Opt. Express* **2010**, *18*, 18592−18597.

(19) Dong, Y.; Yu, G.; McAlpine, M. C.; Lu, W.; Lieber, C. M. *Nano Lett.* **2008**, *8*, 386−391.

(20) Kim, K.-H.; Gaba, S.; Wheeler, D.; Cruz-Albrecht, J. M.; Hussain, T.; Srinivasa, N.; Lu, W. *Nano Lett.* **2012**, *12*, 389−395.

(21) Jo, S. H.; Kim, K.-H.; Lu, W. *Nano Lett.* **2009**, *9*, 870−874.

(22) Jo, S. H.; Lu, W. *Nano Lett.* **2008**, *8*, 392−397.

(23) Sze, S.; Ng, K. *Physics of Semiconductor Devices*; Wiley: New York, 2006.

(24) Ielmini, D.; Zhang, Y. *J. Appl. Phys.* **2007**, *102*, 054517.

(25) Kumar, R. *Electrical Conduction and Dielectric Behaviour of Thin Films of Vacuum Evaporated Amorphous Silicon Hydrogenated Amorphous Silicon and Chemically Deposited Cadmium Sulphide.* Ph.D. Thesis, Cochin University of Science and Technology, Cochin, India, 1990.

(26) Jo, S. H.; Kim, K.-H.; Lu, W. *Nano Lett.* **2009**, *9*, 496−500.

(27) Sebbag, Y.; Goykhman, I.; Desiatov, B.; Nachmias, T.; Yoshaei, O.; Kabla, M.; Meltzer, S. E.; Levy, U. *Appl. Phys. Lett.* **2012**, *100*, 141107.